Hindawi Publishing Corporation
Advances in Materials Science and Engineering
Volume 2014, Article ID 480138, 8 pages
http://dx.doi.org/10.1155/2014/480138

Research Article

Preparation and Characterization of Cetyl Trimethylammonium Intercalated Sericite

Hao Ding,[1] Yuebo Wang,[1] Yu Liang,[1] and Faxiang Qin[2]

[1] *Beijing Key Laboratory of Materials Utilization of Nonmetallic Minerals and Solid Wastes, National Laboratory of Mineral Materials, School of Materials Science and Technology, China University of Geosciences, Beijing 100083, China*
[2] *1D Nanomaterials Group, National Institute for Materials Science, 1-2-1 Sengen, Tsukuba, Ibaraki 305-0047, Japan*

Correspondence should be addressed to Hao Ding; dinghao@cugb.edu.cn

Received 15 August 2014; Accepted 16 October 2014; Published 24 November 2014

Academic Editor: Peter Majewski

Intercalated sericite was prepared by intercalation of cetyl trimethylammonium bromide (CTAB) into activated sericite through ion exchange with the following two steps: the activation of sericite by thermal modification, acid activation and sodium modification; the ion exchange intercalation of CTA^+ into activated sericite. Effects of reaction time, reaction temperature, CTAB quantity, kinds of medium, and aqueous pH on the intercalation of activated sericite were examined by X-ray diffraction (XRD) analysis, Fourier transform infrared (FT-IR) spectroscopy, differential scanning calorimetry (DSC), and thermogravimetric analysis (TGA). The results indicated that the CTA^+ entered sericite interlayers and anchored in the aluminosilicate interlayers through strong electrostatic attraction. The arrangement of CTA^+ in sericite interlayers was that alkyl chain of CTA^+ mainly tilted at an angle about 60° (paraffin-type bilayer) and 38° (paraffin-type monolayer) with aluminosilicate layers. The largest interlayer space was enlarged from 0.9 nm to 5.2 nm. The intercalated sericite could be used as an excellent layer silicate to prepare clay-polymer nanocomposites.

1. Introduction

Clay-polymer nanocomposites, prepared by intercalation of polymers into the interlayer space of phyllosilicates, have attracted much attention for their remarkable improvements in material properties, as compared with virgin polymers or conventional microcomposites and macrocomposites. The improvements include high moduli, increased strength and heat resistance, decreased gas permeability and flammability, and increased biodegradability of biodegradable polymers [1–3]. Clay-polymer nanocomposites have a wide scale of applications in a range of key areas, such as aerospace, automobile, appliance, and electronics waste water treatment [4, 5]. Focusing on the structure of clay-polymer nanocomposites, they can be classified as intercalated nanocomposites and exfoliated nanocomposites. The silicate layers in the former are not fully separated but presented ordered layered structure, compared with the latter [4]. According to the strength of interfacial interactions between the polymer matrix and layered silicate, clay-polymer nanocomposites can also be divided into three types, namely, (a) intercalated nanocomposites: polymer matrix insert into layered silicate in crystallographically regular way, regardless of the ratio of layered silicate to polymer; (b) flocculated nanocomposites: they are almost similar to intercalated nanocomposites except for the silicate layers that are flocculated sometimes due to their hydroxylated edge-edge interaction; (c) exfoliated nanocomposites: the individual layers are separated into a continuous polymer matrix with average distances [1].

According to the number and the ratio of sheets in a fundamental structural layer, the existing cation substitutions in the octahedrons and tetrahedrons, and the resulting charge of the layers, the crystalline clay minerals are classified into seven groups [5, 6]. The common phyllosilicates used for preparation are 2 : 1 type (montmorillonite, vermiculite, and mica) and 1 : 1 type (kaolinite). Montmorillonite [7–12] and vermiculite [13–19] have been mostly investigated as adsorbents for wastewater treatment because of its swelling behavior and excellent ion exchange property. Isomorphous substitution within silicate layers is responsible for the presence of exchangeable cations within the interlamellar region [6, 20]. Phyllosilicates are characterized by moderate surface

Table 1: Chemical composition of the original sericite.

Composition	SiO_2	Al_2O_3	Fe_2O_3	TiO_2	K_2O	Na_2O	CaO	MgO	SO_3	L.O.I	Total
Content (mass %)	45.71	28.32	3.04	0.35	8.09	0.71	0.10	2.12	0.075	4.47	99.555

charge known as the cation exchange capacity (CEC). This charge is not locally constant but varies from layer to layer and must be considered as an average value over the whole crystal [1, 21], while excessive CEC will lead to the instability of interlayer cation and could not serve as the excellent matrix materials for cation modification.

Comparing with other clay minerals, sericite holds the advantages of high moduli, stable chemical property, high electrical insulation, good ultraviolet ray resistance, and so forth [22–24]. Its structure consisted of layers made up of two Si/Al tetrahedral sheets and a sandwiched octahedral sheet filled with Al^{3+} and K^+ (mainly) in interlayer. It also belongs to 2 : 1 phyllosilicates; however, there are a few distinct differences as compared with montmorillonite and vermiculite [5, 25, 26]. It does not swell in water and hardly has ion exchange capacity and intercalation property because of its high layer charge producing pretty strong electrostatic force [27]. The difficult preparation based on sericite explains the lack of literature concerning the intercalation or exfoliation of mica groups compared with montmorillonite and vermiculite.

Intercalated sericite is important to serve as potential sorbents in the removal/speciation of various pollutants in the waste waters and perhaps emerged as a new area of research in the waste water treatment technologies [28, 29]. Cetyltrimethylammonium bromide (CTAB), a typical cationic surfactant, is often used in the modification of clay to increase to adsorption of matrix and also presents heat-resistant, acid and alkali resistance, and bactericidal activity. The treatment and activation of sericite increased the quantity of exchangeable cations, and the organic modification of sericite made the preparation of clay-polymer nanocomposites based on sericite easier. To do this, here we proposed three steps: first, activating the structure of sericite to make it have more exchangeable cations and intercalation properties; second, modifying layered structure of sericite by cation surfactant such as CTAB; third, intercalating polymer into organic sericite interlayers to exfoliate entirely or partly its layers.

In this paper, sericite was activated by thermal modification, acid activation, and sodium modification, and the intercalated sericite was prepared by the intercalation of cetyl trimethylammonium ions (CTA^+) into activated sericite. Reaction time, temperature, quantity of intercalation agent, reaction medium, and pH on intercalation were discussed in sericite intercalation.

2. Materials and Methods

2.1. Materials. The original sericite (S_0) was obtained from Anhui Province, China, whose mean size was about 10 μm. The chemical composition of S_0 was listed in Table 1. Cetyl trimethylammonium bromide (CTAB) with a purity of 99% was provided by Xilong Chem. Co., China, which was used as cation surfactant.

2.2. Preparation. The original powder (S_0) was heated at 800°C in muffle furnace for 1 h. The resulting product (S_1) was stirred with nitric acid of 5 mol/L at 95°C in thermostatic water bath for 4 h, and the product was washed till pH = 7. Then the powder (S_2) was reacted with NaCl supersaturated solution at 95°C for 3 h, and the product was washed and filtrated till without Cl^- (tested by $AgNO_3$). Finally, the activated sericite (S_3) was obtained after drying process. Subsequently, a certain amount of S_3 and the surfactant CTAB were dispersed in distilled water, respectively. The mass ratio S_3/water was 3/100. After mixing the dispersion of S_3 and CTAB solution (by magnetic stirring), the dispersion was heated to 80°C for 24 h and pH was adjusted to neutral and weak acid with HNO_3. And then, the turbid liquid was laid aside for 2 h. After that, the product was washed with distilled water (room temperature) till Br^- removed effectively (tested by $AgNO_3$). The final product (CTA-S) was dried at 80°C.

2.3. Characterization. The X-ray diffraction patterns were obtained on a Rigaku Rotaflex X-ray powder diffractometer, employing Cu Kα radiation, 40 kV, and 100 mA. The X-ray diffraction (XRD) patterns in the 2θ range from 1° to 10° were collected at 0.5°/min. Middle-infrared transmission spectra (500–4000 cm^{-1}) were collected using a Nicolet Magna-IR 750 Fourier transform infrared spectrometer equipped with a Nicolet NicPlan IR Microscope operated with a spectral resolution of 4 cm^{-1}. Simultaneous collecting DSC and TGA signals was carried out using a SDT Q600 analyzer (from TA, the U.S) under air flow and heating the samples from room temperature to 1100°C at 10°C/min. Mass of the samples was about 5 mg.

Sericite does not belong to the clay minerals in the narrow sense, but it is a hydratable layered silicate with a certain layer charge, especially after activation and structure transformation. Cation exchange capacity can be used as a measure of the activity. Ammonium chloride-anhydrous ethanol method was used in this experiment to determine the cation exchange capacity of sericite. The pH value was adjusted to 7 during the measurement.

The intercalation rate, defined as the rate of diffraction peak intensities which can reflect the change of interlayer spacing before and after the layered silicate, is intercalated and can be used to evaluate the degree of intercalation reaction. The intercalation rate can be expressed as follows [31]:

$$\text{I.R} = \frac{I_c}{(I_c + I_k)}, \quad (1)$$

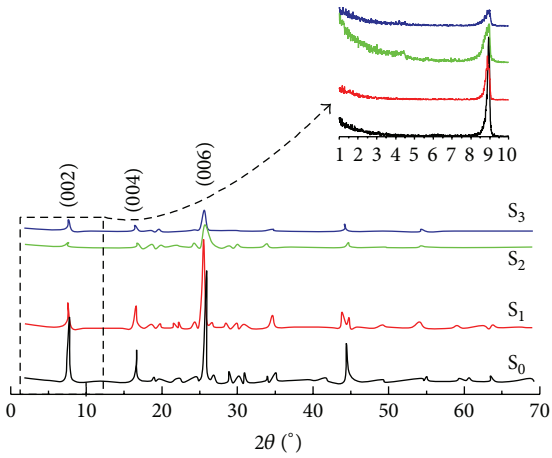

FIGURE 1: XRD patterns of S_0, S_1, S_2, and S_3.

where I_c is intensity of the diffraction peak reflecting the extended interlayer spacing of layer silicate layer after intercalation and I_k is intensity of the diffraction peak reflecting the unextended interlayer spacing of layer silicate layer after intercalation.

The more the extended layer silicate after intercalation, the less the residual unextended layer silicate. As for sericite, the layer spacing is reflected by d_{002} value, so the intercalation rate can be calculated using the intensity of (002) reflection.

3. Results and Discussion

3.1. Characterization of Activated Sericite. The intensities of reflections in Figure 1 decreased and became wider from S_0 to S_3, the reflections corresponding to 2θ moved towards lower degree, and d_{002}-value increased slightly. The intensities of the reflections of S_0 weakened, which moved towards lower 2θ angle region after heat treatment, but they were still sharp and narrow. This was because with the increase of roasting temperature, the lattice of sericite absorbed more energy, and lattice vibration enhanced. Therefore, sericite was activated preliminary. After reacting with nitric acid, the crystallinity of S_2 decreased slightly. However, the layered structure still retained, judging from its 002 reflection existed. It can be concluded that acid activation made S_1 much more activated in crystal lattice without destroying its structure by high concentration of H^+ dissolving part of Al^{3+} at high temperature. Then S_2 reacted with Na^+ for ion exchange, whose hydration radius was smaller than K^+ and provided a CEC of 0.56 meq/g which was much larger than that of S_0, 0.07 meq/g. The relative high cation exchange capacity contributes to the intercalation modification.

3.2. Effects of Reaction Conditions on Intercalation. The basal spacing of S_3 was 0.9 nm. When S_3 and CTAB (15 times the CEC of S_3) were mixed and stirred at 80°C for 10 h or 4 h, the intercalation of CTAB was not observed distinctly except for some protuberances when $2\theta < 5^\circ$ (Figure 3(a)), which indicated that CTAB entered the interlayer spaces with an erratic arrange. When reaction time was extended to 16 h, new basal reflections corresponding to $d_{002} = 4.3$ nm ($2\theta = 2^\circ$) were observed obviously, which suggested that CTAB entered the interlayer spaces with a regular arrange. Moreover, the interlayer spaces of (002) plane were even partly enlarged to 5.2 nm when reaction time was 24 h. The intercalation rate was obtained according to formula (1). The results were 60%, 73%, 76%, and 82%, corresponding to the four times (4 h, 10 h, 16 h, and 24 h). Consequently, with the increase of reaction time, more doses of surfactant entered interlayer spaces and arranged more regularly.

The intercalations at different reaction temperatures were investigated (Figure 3(b)). When temperature was low, lack of energy was afforded in the reaction [32]. And the intensity of new basal reflection (d_{002}) was much weaker than that at higher temperature, as well as the intercalation rate. With the increase of temperature, the interlayer spaces became larger. However, it decreased when temperature was high up to 95°C, because severe high temperature makes CTA^+ too active to be adsorbed and, instead, easily to desorbed from interlayer spaces, which reduced the tendency for ion exchange.

Mechanism of CTA^+ intercalation into sericite interlayers can be described as

$$X^{n+}\text{–S} + n\text{N}^+ \longleftrightarrow n\text{N}^+\text{–S} + X^+, \quad (2)$$

where X is all kinds of inorganic cations taking part in the exchange and N is nitrogen in CTAB.

The CTAB quantity should be much larger than it supposed to be because of the reversible reaction. The right direction is beneficial to the intercalation [33].

The result shown in Figure 4(a) is a proof for the successful intercalation of all the samples with different doses of surfactant. With the increase of the CTAB quantity, the reflection intensities of new basal spaces became stronger and stronger, and the new basal spaces became increasingly larger. Corresponding to 5 times, 10 times, 15 times, and 20 times the CEC of S_3, the intercalation rates were 67%, 69%, 82%, and 64%, respectively. When the quantity of CTAB was 15 times the CEC of S_3, the value of d_{002} was 5.2 nm, the sharp and distinct 002 reflection suggested that CTA^+ in interlayers arranged more regularly than that of others. However, the intercalated effect turned bad when the quantity was 20 times, which was induced by the agglomeration of large quantity of CTAB. The agglomeration decreased the dispersity and hindered the intercalation reaction. Two kinds of medium were considered. Figure 4(b) showed that the reflection of the sample modified with aqueous solution was sharper and stronger than that with n-butanol. A 10% higher intercalated rate was gained using water as the solvent instead of n-butanol. It could be explained by reaction of hydroxy in n-butanol with the interlayer exchangeable cations and/or the broken bonds of the aluminosilicate layers, which reduced the odds for ion exchange of interlayer cations with CTA^+.

The influence of pH value on the intercalation mainly reflects in the ionization of surfactants. The hydrolytic reaction $CTA^+ + H_2O \rightleftharpoons$ CTA-OH $+ H^+$ exists in the reaction medium. According to the equation, the addition of H^+ restrains the reaction and thus produces more CTA^+ in the system, which facilitates the intercalation; on the contrary,

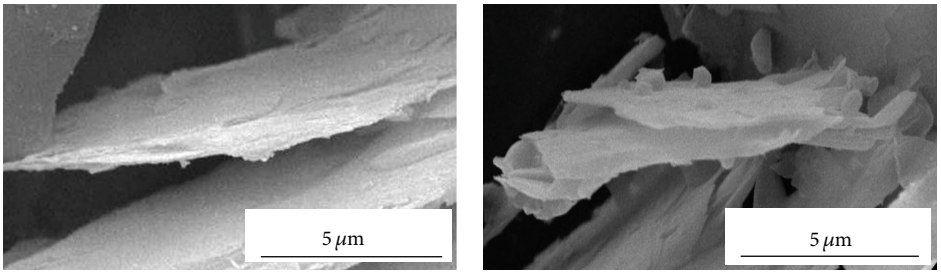

Figure 2: SEM images of sericite (a) before and (b) after intercalation.

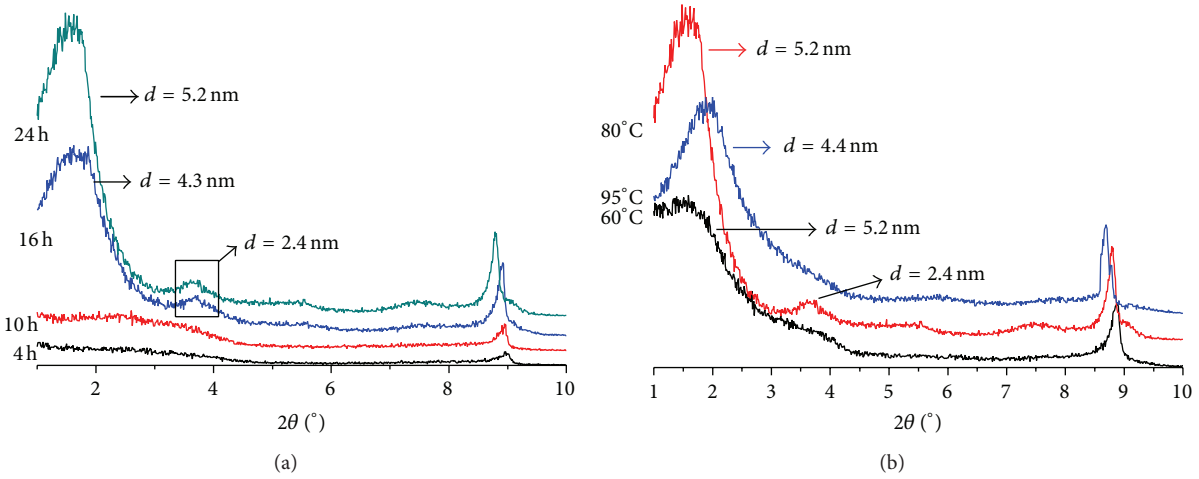

Figure 3: XRD patterns of CTA-S reaction for different (a) time and (b) temperatures.

alkaline environment promotes the hydrolysis, resulting in reduced reaction rate. From this perspective, the acidic environment is conducive to the intercalation.

Five different pH values of reaction medium were adjusted to investigate the effect of pH value on the intercalation effect. The results shown in Figure 5 indicated that sericite was intercalated in neutral and weak acid aquatic solution. When pH value of the reaction medium was 1, nearly no new reflection was observed and even the original peak almost disappeared, which was a proof of an unsuccessful intercalation. This was because the strong acid destroyed the structure of sericite, thus leading to a poor result of intercalation. In the case of intercalation at pH 4 and 7, S_3 was intercalated well and new basal reflection was obtained (Figure 5). In the alkaline medium (pH 9 and 11), no new basal reflection appeared, and in that the quantity of CTA^+ was too little to intercalate S_3, though alkaline medium was benefit for the dispersing of sericite.

3.3. Characterization of Modified Sericite. The FT-IR spectra of original sericite (S_0), pure CTAB, and intercalated sericite (CTA-S, the one preparing at optimal conditions) were given in Figure 6. The spectra of CTA-S (Figure 6(c)) showed that two new bands at 2918 cm^{-1} and 2849 cm^{-1} appeared which were assigned to the CH_2 asymmetric and symmetric stretching vibration. The band of Si–O stretching vibration (1024 cm^{-1}) was wider and weaker than that of S_0 (Figure 6(a)), which could be assigned to the appearance of the band of C–N and C–C bending vibration (962 cm^{-1} and 909 cm^{-1}). The band at 720 cm^{-1} was diagnostic of linear alkyl chain $-(CH_2)_n-$ when $n > 4$, whose disappearance after the intercalation of modified sericite indicated that alkyl chains were in interlayers with a twisted shape. When CTA^+ entered the interlayer of sericite, the shape of alkyl chain twisted to a certain extent due to the impact of two adjacent layers. It was considered that crook of alkyl chain had little effect on its length in interlayer. According to the reflections in XRD patterns of CTA-S (the topper one shown in Figure 4(b)) and the results mentioned above, it could be concluded that CTA^+ entered sericite interlayer and the intercalation was stable due to the strong electrostatic force between CTA^+ and layer.

The DSC-TGA curves of S_0 and CTA-S were shown in Figure 7, respectively. There was only one mass loss in the TGA curve for S_0 at 4.89% at 1100°C (Figure 7(a)) according to the DSC curve peak at the same temperature. This mass loss was attributed to the loss of structural water of S_0. Displayed in thermogravimetric curves of Figures 7(b), 7(c), and 7(d), the mass loss of organic modified sericite increased with the increase of the dosage of CTAB. When the dosage of CTAB was 15 CEC, the mass loss reached 13.61%. Subtracting the 4.89% interlayer water contained in sericite

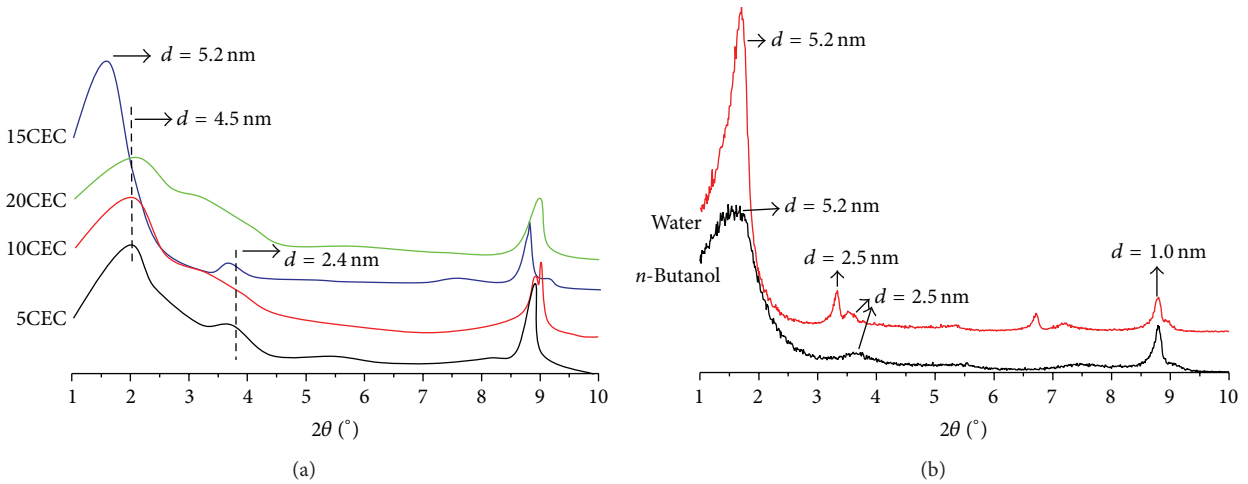

Figure 4: XRD patterns of CTA-S reaction with different (a) quantities of CTAB and (b) mediums.

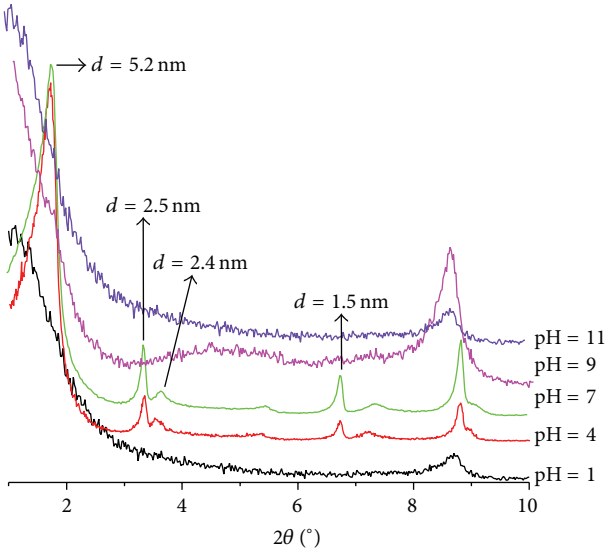

Figure 5: XRD patterns of CTA-S reaction with different pH.

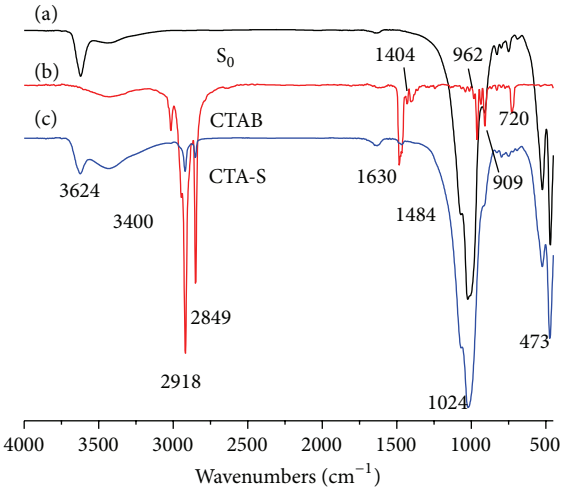

Figure 6: FT-IR spectra of (a) S_0, (b) CTAB, and (c) CTA-S.

raw materials, it could be considered that 8.72% of the CTAB was in the sericite. As for the DSC of CTA-S, there were three endothermic valleys at 100°C, 200°C~250°C, and 900°C and two obvious exothermic peaks at 250°C~300°C and 250°C~400°C. After modification, temperature of the first endothermic valley was slightly lower than the original one. This change indicated that the CTAB went into the sericite interlayer through intercalation. Then the sericite slice layer surface transformed from hydrophilic to hydrophobic makes the adsorption capacity of water molecules weaken and, therefore, the desorption temperature of interlayer water lower.

Analysis of FT-IR spectra and DSC-TGA curves indicated that intercalator is inserted into sericite interlayer by means of chemical reaction. The maximum intercalation capacity can reach to 8.72% and firm chemical bond was formed between CTAB and sericite layer.

3.4. Microstructures of Modified Sericite. There were two ideas about the arrangement of alkyl chains in interlayers of layered silicates. One was that the alkyl chains either lay parallel to the aluminosilicate layers forming mono or bilayers or radiate away from the layers forming mono or bimolecular arrangements [34]. The other was that, as for short chain lengths, the molecules were effectively isolated from each other; for medium lengths, there is various degree of disorder in plane and interdigitation between layers; for long lengths, interlayer order increased leading to a liquid-crystalline polymer [35]. It was also considered that, with the increase of CTAB concentration, the tail of CTA^+ chain began to radiate away from the aluminosilicate surface and the head groups distributed on aluminosilicate layers uniformly, and the chains of CTA^+ adopt highly ordered arrangement with a fully stretched all-trans conformation. Furthermore, according to the viewpoint of Zhu et al. [36], there were six typical arrangements of alkyl chain in interlayer, which

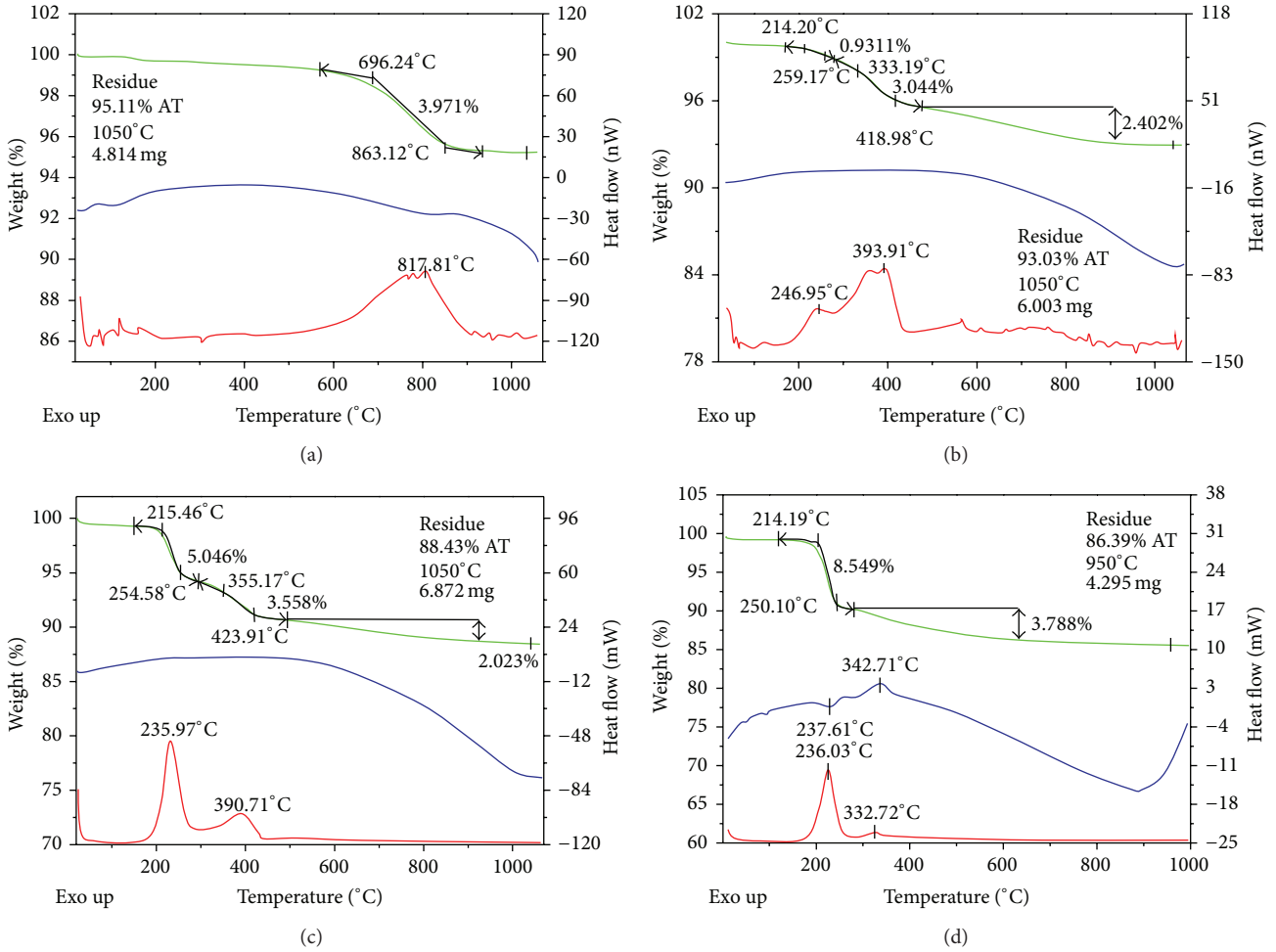

FIGURE 7: DSC-TGA curves and integral curves of TGA of S_0 (a) and CTA-S modified by different quantities of CTAB (5 CEC (b), 10 CEC (c), and 15 CEC (d)).

were lateral-monolayer ("L" type and "M" type), lateral-bilayer, paraffin-type monolayer, pseudotrilayer and paraffin-type bilayer. The contrastive SEM images of sericite before (Figure 2(a)) and after (Figure 2(b)) intercalation indicated that the sericite slice layer was partly dispersed and stripped after intercalation modification. The disperse and exfoliate extent were not well-proportioned, which corresponded to the previous analysis results that intercalators distribute between the layers in a variety of forms.

The schematic drawing about the size of CTA^+ was shown in Figure 8. By synthesizing the points of views above, we illustrate the CTA-S prepared in aqueous (the upper one shown in Figure 4(b)) as an example.

There were five major reflections in its XRD pattern. The d-value according to the first reflection was 5.2 nm, which can be explained that some of the CTA^+ chains were full stretched and orderly tilted at an angle of 60° (Figure 9). The d-values associated with the second and the third reflection were 2.5 nm and 2.4 nm, respectively, which could be explained by the fact that some of CTA^+ chains were arranged in the type of paraffin-type monolayer at an angle of 38°. The d-value of

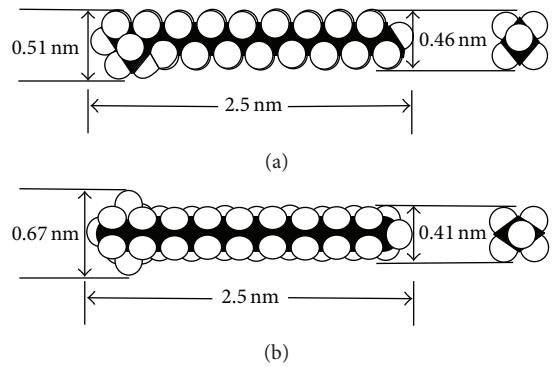

FIGURE 8: The schematic drawing about the size of CTA^+: (a) side view and (b) top view [30].

the forth reflection was 1.2 nm, which was lesser than that of lateral-monolayer. Therefore, of the second reflection in Figure 4(b) was of the second order. The appearance of the last reflection evidenced the vestigial of S_3. In other words, S_3 was not be modified completely in reaction.

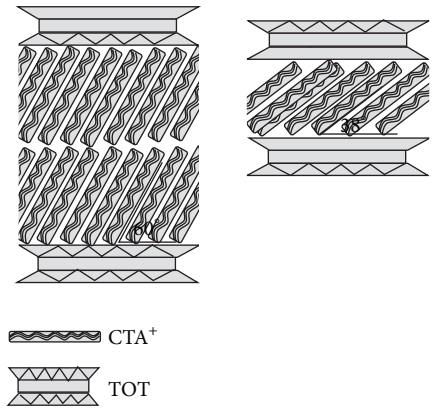

Figure 9: The schematic drawing about the arrangement of CTA^+ in the interlayer of CTA-S.

4. Conclusions

Intercalated sericite was prepared by CTA^+ intercalating into activated sericite. The best intercalated sericite, in which CTA^+ enlarged the basal spacing from 0.9 nm to 5.2 nm, was prepared under reaction time of 24 h, reaction temperature of 80°C, CTAB quantity of 15 times (by mol) of sericite (according to CEC), and reaction medium of aqueous with pH = 4. The results shown by FT-IR, DSC and TG proved that about half of CTA^+ physisorbed on the surface of CTA-S, and the rest entered the sericite interlayers and stayed stably. The arrangements of CTA^+ in sericite interlayers were constituted by the CTA^+ chains mainly tilted at an angle about 60° (paraffin-type bilayer) and 38° (paraffin-type monolayer) with layers.

Conflict of Interests

The authors declare that there is no conflict of interests regarding the publication of this paper.

Acknowledgment

The authors would like to acknowledge the Fundamental Research Funds for the Central Universities (2011PY0169) for financial support during part of this research.

References

[1] S. Sinha Ray and M. Okamoto, "Polymer/layered silicate nanocomposites: a review from preparation to processing," *Progress in Polymer Science*, vol. 28, no. 11, pp. 1539–1641, 2003.

[2] C. Zhao, H. Qin, F. Gong, M. Feng, S. Zhang, and M. Yang, "Mechanical, thermal and flammability properties of polyethylene/clay nanocomposites," *Polymer Degradation and Stability*, vol. 87, no. 1, pp. 183–189, 2005.

[3] H. Qin, Q. Su, S. Zhang, B. Zhao, and M. Yang, "Thermal stability and flammability of polyamide 66/montmorillonite nanocomposites," *Polymer*, vol. 44, no. 24, pp. 7533–7538, 2003.

[4] S. Pavlidou and C. D. Papaspyrides, "A review on polymer-layered silicate nanocomposites," *Progress in Polymer Science (Oxford)*, vol. 33, no. 12, pp. 1119–1198, 2008.

[5] S. M. Lee and D. Tiwari, "Organo and inorgano-organo-modified clays in the remediation of aqueous solutions: an overview," *Applied Clay Science*, vol. 59-60, pp. 84–102, 2012.

[6] J. Konta, "Clay and man: clay raw materials in the service of man," *Applied Clay Science*, vol. 10, no. 4, pp. 275–335, 1995.

[7] U. C. Ugochukwu, D. A. C. Manning, and C. I. Fialips, "Effect of interlayer cations of montmorillonite on the biodegradation and adsorption of crude oil polycyclic aromatic compounds," *Journal of Environmental Management*, vol. 142, pp. 30–35, 2014.

[8] Z. Qin, P. Yuan, S. Yang, D. Liu, H. He, and J. Zhu, "Silylation of Al_{13}-intercalated montmorillonite with trimethylchlorosilane and their adsorption for Orange II," *Applied Clay Science*, vol. 99, pp. 229–236, 2014.

[9] S. Yang, M. Gao, and Z. Luo, "Adsorption of 2-naphthol on the organo-montmorillonites modified by Gemini surfactants with different spacers," *Chemical Engineering Journal*, vol. 256, pp. 39–50, 2014.

[10] R. Zhang, W. Yan, and C. Jing, "Mechanistic study of PFOS adsorption on kaolinite and montmorillonite," *Colloids and Surfaces A*, vol. 462, pp. 252–258, 2014.

[11] R. Ait-Akbour, P. Boustingorry, F. Leroux, F. Leising, and C. Taviot-Guého, "Adsorption of PolyCarboxylate Poly(ethylene glycol) (PCP) esters on Montmorillonite (Mmt): effect of exchangeable cations (Na^+, Mg^{2+} and Ca^{2+}) and PCP molecular structure," *Journal of Colloid and Interface Science*, vol. 437, pp. 227–234, 2015.

[12] I. Perassi and L. Borgnino, "Adsorption and surface precipitation of phosphate onto $CaCO_3$–montmorillonite: effect of pH, ionic strength and competition with humic acid," *Geoderma*, vol. 232–234, pp. 600–608, 2014.

[13] X. Ren, Z. Zhang, H. Luo et al., "Adsorption of arsenic on modified montmorillonite," *Applied Clay Science*, vol. 97-98, pp. 17–23, 2014.

[14] F. H. Do Nascimento and J. C. Masini, "Influence of humic acid on adsorption of Hg(II) by vermiculite," *Journal of Environmental Management*, vol. 143, pp. 1–7, 2014.

[15] A. Sarı and M. Tüzen, "Adsorption of silver from aqueous solution onto raw vermiculite and manganese oxide-modified vermiculite," *Microporous and Mesoporous Materials*, vol. 170, pp. 155–163, 2013.

[16] T. Hongo, S. Yoshino, A. Yamazaki, A. Yamasaki, and S. Satokawa, "Mechanochemical treatment of vermiculite in vibration milling and its effect on lead (II) adsorption ability," *Applied Clay Science*, vol. 70, pp. 74–78, 2012.

[17] Z.-D. Wen, D.-W. Gao, Z. Li, and N.-Q. Ren, "Effects of humic acid on phthalate adsorption to vermiculite," *Chemical Engineering Journal*, vol. 223, pp. 298–303, 2013.

[18] H. Long, P. Wu, L. Yang, Z. Huang, N. Zhu, and Z. Hu, "Efficient removal of cesium from aqueous solution with vermiculite of enhanced adsorption property through surface modification by ethylamine," *Journal of Colloid and Interface Science*, vol. 428, pp. 295–301, 2014.

[19] E. Padilla-Ortega, R. Leyva-Ramos, and J. Mendoza-Barron, "Role of electrostatic interactions in the adsorption of cadmium(II) from aqueous solution onto vermiculite," *Applied Clay Science*, vol. 88-89, pp. 10–17, 2014.

[20] S. W. Bailey, "Interstratified clay minerals," in *Crystal Structure of Clay Minerals and Their X-Ray Identification*, G. W. Brndley and G. Brown, Eds., pp. 1–113, Mineralogical Society, London, UK, 1980.

[21] M. Alexandre and P. Dubois, "Polymer-layered silicate nanocomposites: preparation, properties and uses of a new class of materials," *Materials Science and Engineering R: Reports*, vol. 28, no. 1, pp. 1–63, 2000.

[22] H. Ding, X. Xu, N. Liang, and Y. Wang, "Preparation sericite nanoflakes by exfoliation of wet ultrafine grinding," *Advanced Materials Research*, vol. 178, pp. 242–247, 2011.

[23] Y.-J. Shih and Y.-H. Shen, "Swelling of sericite by $LiNO_3$-hydrothermal treatment," *Applied Clay Science*, vol. 43, no. 2, pp. 282–288, 2009.

[24] R. A. Vaia, R. K. Teukolsky, and E. P. Giannelis, "Interlayer structure and molecular environment of alkylammonium layered silicates," *Chemistry of Materials*, vol. 6, no. 7, pp. 1017–1022, 1994.

[25] F. Bergaya and G. Lagaly, "Mechanical properties of clays and clay minerals," in *Developments in Clay Science. Handbook of Clay Science*, vol. 1, pp. 274–260, Elsevier, Amsterdam, The Netherlands, 2006.

[26] H. W. Ma, *Industrial Minerals and Rocks*, Chemical Industry Press, Beijing, China, 3rd edition, 2011.

[27] X. F. Yu, B. Ram, and X. C. Jiang, "Parameter setting in a bio-inspired model for dynamic flexible job shop scheduling with sequence-dependent setups," *European Journal of Industrial Engineering*, vol. 1, no. 2, pp. 182–199, 2007.

[28] D. Tiwari and S. M. Lee, "Novel hybrid materials in the remediation of ground waters contaminated with As(III) and As(V)," *Chemical Engineering Journal*, vol. 204-205, pp. 23–31, 2012.

[29] S.-M. Koh and J. B. Dixon, "Preparation and application of organo-minerals as sorbents of phenol, benzene and toluene," *Applied Clay Science*, vol. 18, no. 3-4, pp. 111–122, 2001.

[30] R. Zhu, L. Zhu, J. Zhu, and L. Xu, "Structure of cetyltrimethylammonium intercalated hydrobiotite," *Applied Clay Science*, vol. 42, no. 1-2, pp. 224–231, 2008.

[31] L. J. Wang, X. L. Xie, N. C. Chen, and C. J. Hu, "Evaluation of kaolinite intercalation efficiency," *Chinese Journal of Inorganic Chemistry*, vol. 26, pp. 853–859, 2010.

[32] Q. M. Ye and X. F. Liu, "Analysis of the microstructure of the CTMAB modified organobentonite," *Bulletin of the Chinese Ceramic Society*, vol. 5, pp. 40–43, 2004.

[33] Z. M. Cui, L. B. Liao, G. M. Chen, and M. S. Yang, "Organic intercalation, polymerization and exfoliation of different montmorillonites," *Journal of the Chinese Ceramic Society*, vol. 33, no. 5, pp. 599–603, 2005.

[34] S. Xu and S. A. Boyd, "Alternative model for cationic surfactant adsorption by layer silicates," *Environmental Science and Technology*, vol. 29, no. 12, pp. 3022–3028, 1995.

[35] R. L. Virta, "Talc and pyrophyllite," *The American Ceramic Society Bulletin*, vol. 84, pp. 25–26, 2005.

[36] J. Zhu, H. He, J. Guo, D. Yang, and X. Xie, "Arrangement models of alkylammonium cations in the interlayer of HDTMA + pillared montmorillonites," *Chinese Science Bulletin*, vol. 48, no. 4, pp. 368–372, 2003.